Front. Optoelectron. 2012, 5(1): 63–67
DOI 10.1007/s12200-012-0184-y

RESEARCH ARTICLE

Effect of dipole location on profile properties of symmetric surface plasmon polariton mode in $Au/Al_2O_3/Au$ waveguide

Gongli XIAO[1,2], Xiang JI[1], Linfei GAO[1], Xingjun WANG[1], Zhiping ZHOU (✉)[1]

1 The State Key Laboratory of Advanced Optical Communication Systems and Networks, School of Electronics Engineering and Computer Science, Peking University, Beijing 100871, China
2 Information and Communications College, Guilin University of Electronic Technology, Guilin 541004, China

Abstract This study uses a dipole embedded in Al_2O_3 layer to excite a symmetric surface plasmon polariton (SPP) mode in $Au/Al_2O_3/Au$ waveguide to investigate its profile properties by using finite-difference time-domain (FDTD) method. The excited dipole decay radiatively direct near-field coupling to SPP mode owing to thin Al_2O_3 layer of 100 nm. The effects of electric and magnetic field intensity profiles and decay length have been considered and characterized. It is found that dipole location is an important factor to influence the horizontal and vertical profile properties of symmetric SPP mode in $Au/Al_2O_3/Au$ waveguide. The amplitudes of electric and magnetic field intensity and the wavelengths of metal-insulator-metal (MIM) SPP resonance mode can be tuned by varying dipole location. The horizontal and vertical decay lengths are 19 and 24 nm, respectively. It is expected that the $Au/Al_2O_3/Au$ waveguide structure is very useful for the practical applications of designing a SPP source.

Keywords waveguide, surface plasmon polariton (SPP), profile properties

1 Introduction

Surface plasmon polariton (SPP) is electromagnetic waves coupled to free electron oscillation on metal surface and propagates along the metal-dielectric interface with the amplitudes decaying into both sides exponentially [1]. One of the most attractive aspects of SPP is the way in which they help concentrate and channel light beyond diffraction limit [2]. Some novel photonic devices based on SPP, such as waveguide [3], reflector [4] and beam splitters [5], have gained an increasing research interest recently. Of available SPP waveguides, metal-insulator-metal (MIM) configuration [6–10] is very promising for compact photonic integration. This is the reason that such a MIM geometry serves as a plasmonic slot waveguide, "squeezing" the SPP field into the dielectric core [11]. Until now, different MIM SPP waveguide have been demonstrated, such as various passive (e.g., filters [12]) and active plasmonic devices (e.g., emitters [13]).

In recent years, the excitation of SPP has been a promising way to squeeze optical energy in nanometric cross section [14]. There are a lot of literatures on SPP excitation, such as electron-induced [15] or light-induced [16] SPP excitation. As the insulator layer of MIM waveguide is too thin to support photonic modes, the excited dipole decay radiatively only by direct near-field coupling to plasmonic transverse magnetic (TM) modes. So, the MIM waveguide geometry is particularly promising for light-induced SPP excitation. Most recently, the SPP sources based on MIM waveguide have been demonstrated experimentally, including an electrical source of SPP using organic semiconductors by Koller et al. [17] and using silicon nanocrystals embedded in Al_2O_3 by Walters et al. [18]. Although the pioneering work [18] already observed and testified that the SPP mode can occur in the MIM waveguide under a certain condition, they did not offer physical origin of such a MIM SPP mode theoretically and an exact condition for its existence. Moreover, the physical origin of such a MIM SPP mode and the exact condition for its existence have important theoretical reference value for the design of a SPP source. However, these vital electromagnetic filed profile properties of SPP mode have been left untouched. It is also noticed that the numerical study of the light (dipole)-induced SPP excitation is an area in urgent need of further work.

Received August 13, 2011; accepted September 6, 2011

E-mail: zjzhou@pku.edu.cn

In this paper, we present the first study of horizontal and vertical profile properties of symmetric SPP mode in Au/Al_2O_3/Au waveguide, which only supports tightly confined coupled SPP mode within the thin Al_2O_3 layer by using finite-difference time-domain (FDTD) method. The aim of this paper is to give a numerical analysis of light (dipole)-induced SPP excitation. Attention will be focused on the fundamental physics and the electromagnetic field profile properties of MIM SPP mode. The simulation results show that both the amplitudes of electric and magnetic field intensity and the wavelengths of MIM SPP resonance mode can be tuned by varying dipole location, owing to the role of coupling between dipole and Au/Al_2O_3/Au waveguide. This phenomenon may provide guidance in designing a SPP source by using Au/Al_2O_3/Au waveguide structure.

2 Theoretic model and FDTD modeling method

MIM waveguide is composed of two identical Au films (200 nm) separated by an insulator layers Al_2O_3 (100 nm), and the horizontal length of the MIM waveguide is infinite, as shown in Fig. 1. When the width (w) of dielectric layer is reduced below the diffraction limit, conventional guiding modes cannot exist. In this case, a TE 90 polarization incident light (dipole) will be transformed into the coupled SPP on the metal surfaces and propagates along the waveguide. The dispersion relation of the SPP in the MIM waveguide can be deduced from the Maxwell equations as [19]

$$\frac{p\varepsilon_{\mathrm{d}}}{k\varepsilon_{\mathrm{m}}} = \frac{1-\mathrm{e}^{kw}}{1+\mathrm{e}^{kw}}, \tag{1}$$

where

$$k = k_0\sqrt{\left(\frac{\beta_{\mathrm{SPP}}}{k_0}\right)^2 - \varepsilon_{\mathrm{d}}}, \tag{2}$$

$$p = k_0\sqrt{\left(\frac{\beta_{\mathrm{SPP}}}{k_0}\right)^2 - \varepsilon_{\mathrm{m}}}, \tag{3}$$

and

$$\beta_{\mathrm{SPP}} = n_{\mathrm{eff}}k_0, \tag{4}$$

where k_0 is the wave vector in free space, β_{SPP} and n_{eff} are the complex propagation constant and the effective refractive index of SPP, respectively. ε_{m} and ε_{d} are the relative dielectric constant of the metal and the dielectric material, respectively. Gold for the metallic cladding layers is characterized by the Drude model [20]

$$\varepsilon_{\mathrm{m}} = 1 - \frac{\omega_{\mathrm{p}}^2}{\omega(\omega+\mathrm{i}\gamma)}, \tag{5}$$

where $\omega_{\mathrm{p}} = 1.2\times10^{16}$ Hz and $\gamma = 1.2\times10^{14}$ Hz are the bulk plasma and damping frequencies, respectively, and Al_2O_3 with refractive index $n_{\mathrm{d}} = 1.7$. As Al_2O_3 layer is too thin (100 nm) to support photonic modes, the excited dipole decay radiatively only by direct near-field coupling to a symmetric SPP mode, which is highly confined within the insulating region. The characteristic equation of symmetric SPP mode is given by [21]:

$$\frac{\kappa_{\mathrm{m}}}{\varepsilon_{\mathrm{m}}} + \frac{\kappa_{\mathrm{d}}}{\varepsilon_{\mathrm{d}}}\tanh\left(\frac{1}{2}\kappa_{\mathrm{d}}w\right) = 0, \tag{6}$$

where $\kappa_{\mathrm{m}} = \sqrt{\beta_{\mathrm{SPP}}^2 - \varepsilon_{\mathrm{m}}}$ and $\kappa_{\mathrm{d}} = \sqrt{\beta_{\mathrm{SPP}}^2 - \varepsilon_{\mathrm{d}}}$ denote the transverse wavenumber of the plasmonic mode in the metal and dielectric, respectively.

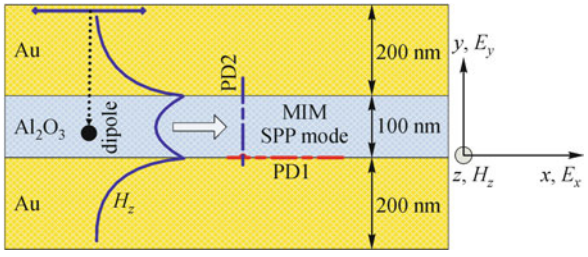

Fig. 1 Schematic structure of proposed Au/Al_2O_3/Au waveguide composed of two identical Au films separated by an insulator layers Al_2O_3, and a dipole is embedded in Al_2O_3 layer to excite a MIM SPP mode for forward propagating

Au/Al_2O_3/Au waveguide two dimensional (2D) structure is designed and modeled by a commercial FDTD package[1)] that supports ununiform meshing and eigenmode calculation. Spatial mesh cells are set to $\Delta x = \Delta y = 5$ nm and the time step is taken as $\Delta t = \Delta s/2c = 8.3333\times10^{-18}$ s. The 2D FDTD method with perfectly matched layer (PML) as boundary condition is used in this work. The fundamental TM mode (E_x;E_y;H_z) of the Au/Al_2O_3/Au waveguide is excited by a dipole source being located in the intermediate Al_2O_3 layer and the mesh grid size is set to 1 nm in order to maintain convergence. And then the MIM SPP mode is excited and two different power monitors PD1 (horizontal) and PD2 (vertical) are set to detect the incident power A1. In this simulation experiment, the dipole in the proposed waveguide structure is located in Al_2O_3 at distances of 10, 15, 20, 25, 30, 35, 40, 45 and 50 nm from the bottom Al_2O_3/Au interface and the thickness of Al_2O_3 is fixed at 100 nm. It is obvious that there is a symmetric plasmonic Hz mode (as shown in Fig. 1) supported in the MIM SPP mode, which arises from an asymmetric coupling of SPP at inner interfaces of Au

1) The commercial software FDTD solutions was employed for the numerical simulation

layers. The simulated electric field and magnetic field intensity profiles of MIM SPP mode with different MIM geometry ($t_{Au(top)} = t_{Au(bottom)} = 200$ nm, $w = 100$ nm) by changing the dipole distance are shown in Figs. 2(a) and 3(a).

3 Simulation results and discussion

To study the influence of dipole location on the performance of symmetric SPP mode in Au/Al_2O_3/Au waveguide, the horizontal profiles of the electric field and magnetic field intensity profiles are calculated for the structures as shown in Figs. 2(a) and 3(a). Figure 2(a) shows the horizontal profiles of the electric field intensity (i_E^x) of MIM SPP mode at the interface of Al_2O_3/Au along the x-axis for the frequency corresponding to the free space wavelength of dipole from 0.6 to 1.8 μm. In addition, the amplified part of MIM SPP resonance model is shown in the inset. By varying dipole distances from 10 to 50 nm in steps of 5 nm with the thickness of Al_2O_3 layer of 100 nm,

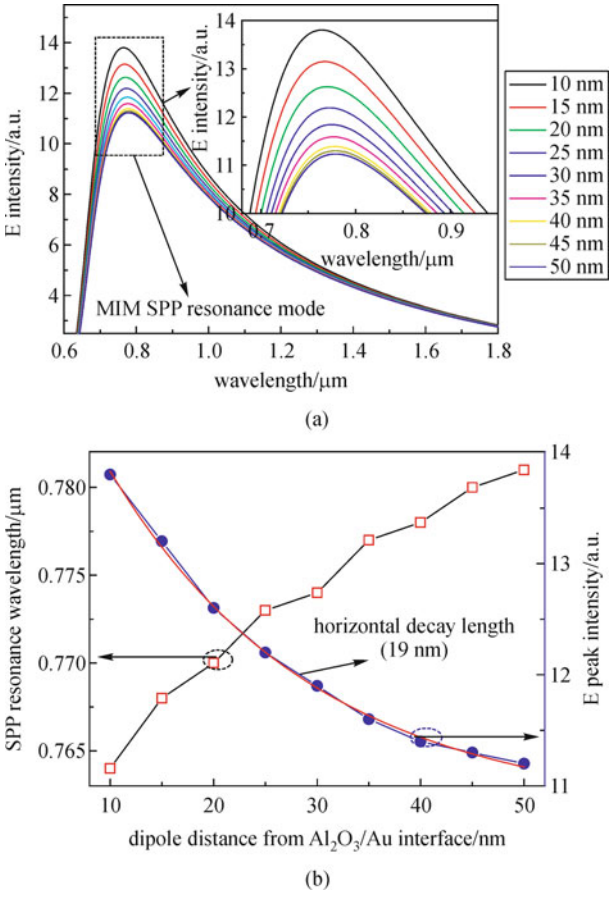

Fig. 2 (a) Horizontal profiles of electric field (E) intensity at bottom Al_2O_3/Au interface as a function of dipole distance; (b) electric (E) field peak intensity and SPP resonance wavelength as function of dipole distance

i_E^x is decreased, due to the different coupling strengths between dipole and Au/Al_2O_3/Au waveguide. This is the reason that dipole distance is critical to the SPP coupling strength. As the dipole distance gets larger, the SPP coupling strength becomes weaker, leading to decrease of i_E^x. In addition, we have plotted two curves based on the data from i_E^x of MIM SPP resonance mode. i_E^x and SPP resonance wavelength (λ_{SPP}) as a function of dipole distance are shown in Fig. 2(b). It is clearly seen that λ_{SPP} is red shifted consistently and i_E^x is exponential decay. The exponential relationship between i_E^x and the dipole distance (d) becomes obvious. i_E^x can be fitted using a exponential function to determine the horizontal decay properties of SPP mode along the x-axis. The fitting curve of the FDTD simulation results for i_E^x is $i_E^x = 5\exp(-d/19) + 11$. So, the horizontal decay length is 19 nm. The physical concept of the horizontal decay length arises from the fact that the change of dipole distance resulting in i_E^x being diminished by 1/e. This is very useful for designing an SPP source with a desirable luminescence center (19 nm) by merely adjusting dipole distance to make best SPP coupling between top and bottom Au films in Au/Al_2O_3/Au waveguide. The redshift of λ_{SPP} with the augment of dipole distances results from the asymmetric coupling of SPP between dipole and Au/Al_2O_3/Au waveguide. It is the reason that the asymmetric coupling of SPP becomes strong when the location of dipole is near the middle position.

Figures 3(a) shows the horizontal profiles of the magnetic field intensity (i_H^x) of MIM SPP mode at the interface of Al_2O_3/Au along the x-axis. i_H^x is also decreased. As the dipole distance gets larger, the SPP coupling strength becomes weaker which results in a decrease of i_H^x. i_H^x and λ_{SPP} as a function of dipole distance are shown in Fig. 3(b). It is clearly seen that λ_{SPP} is red shifted consistently and i_H^x is exponential decay. The fitting curve of the FDTD simulation results for i_H^x is $i_H^x = 2.4 \times 10^{-4}\exp(-d/19) + 5.7 \times 10^{-4}$. The horizontal decay length is 19 nm.

To achieve an in-depth understanding of the effect of dipole distance on the profile properties of MIM SPP mode, we used a 2D FDTD numerical simulation to model the vertical profiles of the electric field and magnetic field intensity of the corresponding MIM SPP resonance mode, as shown in Figs. 4 and 5 along the y-direction. Figure 4 shows the vertical profiles of the electric field intensity (i_E^y) of the corresponding MIM SPP resonance mode along the y-axis. i_E^y is decreased exponentially with increasing the dipole distance from 10 to 50 nm in steps of 5 nm, due to the SPP coupling strength becoming weaker. The MIM SPP resonance mode effect clearly appears at vertical profiles along the y-axis (peak and dip). Furthermore, the positions of peaks and dips in the electric field intensity profiles are almost not affected, which are centered around ±0.044 and 0 μm, respectively, and the width between dips

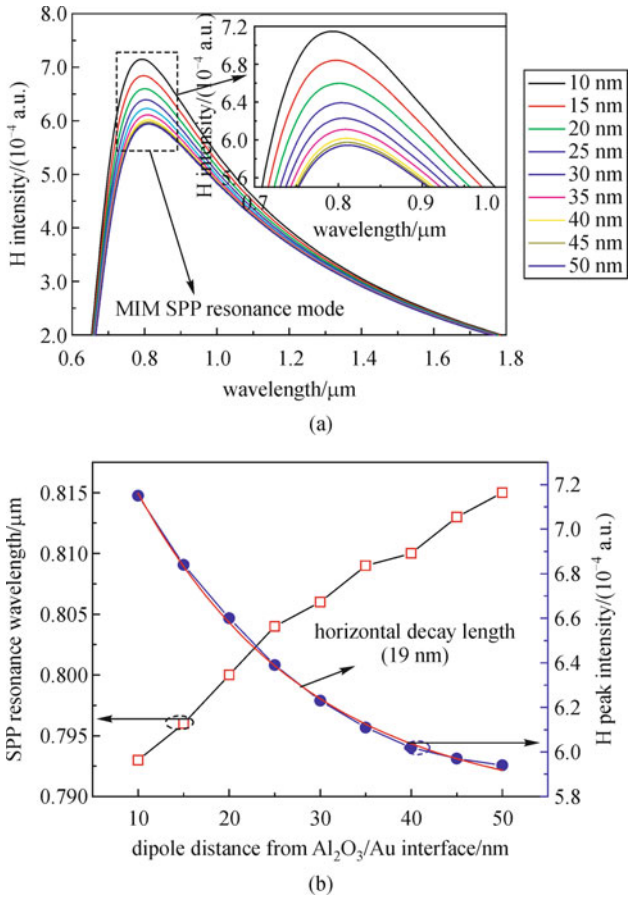

Fig. 3 (a) Horizontal profiles of magnetic field (H) intensity at bottom Al_2O_3/Au interface as function of dipole distance; (b) magnetic field (H) peak intensity and SPP resonance wavelength as function of dipole distance

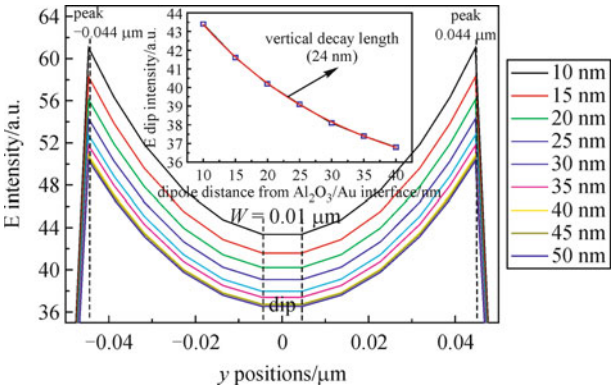

Fig. 4 Vertical profiles of electric field (E) intensity of corresponding MIM SPP resonance mode along *y*-axis as function of dipole distance. Inset, dependence of electric field dip intensity on dipole distances

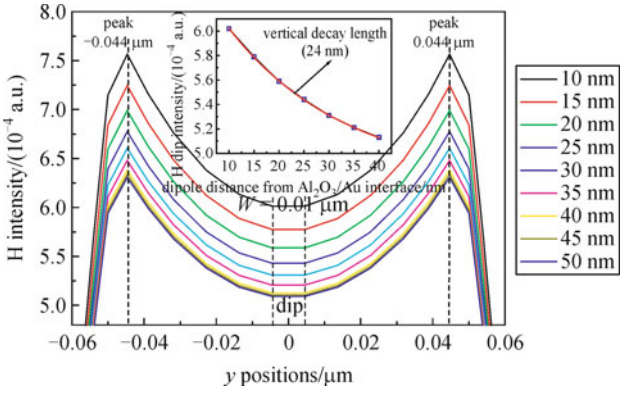

Fig. 5 Vertical profiles of magnetic field (H) intensity of corresponding MIM SPP resonance mode along *y*-axis as function of dipole distance. Inset, dependence of magnetic field dip intensity on dipole distances

is 0.01 μm. In addition, the exponential relationship between i_E^y and d becomes obvious as shown in the inset. i_E^y can be fitted using a exponential function to determine the vertical decay properties of SPP mode in the Au/Al_2O_3/Au MIM waveguide along the *y*-axis. The fitting curve of the FDTD simulation results for i_E^y is $i_E^y = 14\exp(-d/24) + 34$. So, the vertical decay length is 24 nm. The physical concept of the vertical decay length arises from the fact that the change of dipole distance resulting in i_E^y being diminished by 1/e. This is very useful for the designing a SPP source with a desirable luminescence center (24 nm) by merely adjusting the locations of dipole to make the coupled SPP model being more gathered and propagated in Al_2O_3 layer.

Figure 5 shows the vertical profiles of the magnetic field intensity (i_H^y) of the corresponding MIM SPP resonance mode along the *y*-axis. i_H^y is also decreased exponentially with increasing the dipole distance from 10 to 50 nm in steps of 5 nm, due to the SPP coupling strength becoming weaker. Furthermore, the positions of peaks and dips in the magnetic field intensity profiles are almost not affected, which are centered around ±0.044 and 0 μm, respectively, and the width between dips is 0.01 μm. The exponential relationship between i_H^y and d becomes obvious as shown in the inset. The fitting curve of the FDTD simulation results for i_H^y is $i_H^y = 1.9 \times 10^{-4}\exp(-d/24) + 4.8 \times 10^{-4}$. So, the vertical decay length is 24 nm.

4 Conclusions

In conclusion, the horizontal and vertical profile properties of symmetric SPP mode in Au/Al_2O_3/Au MIM waveguide are investigated by varying dipole location yet the thickness of Al_2O_3 layer being fixed at 100 nm through the FDTD simulation. Based on the calculated electromagnetic field intensity profile properties, the dipole

location is an important factor to the horizontal and vertical profile properties of symmetric SPP mode. The horizontal profiles of i_E^x and i_H^x decrease and λ_{SPP} are red shifted consistently when the dipole distances increase. The vertical profiles of i_E^y and i_H^y are also decreased exponentially with increase of the dipole distances. However the positions of peaks and dips in the electric field and magnetic field intensity are not affected. The horizontal and vertical decay lengths are 19 and 24 nm respectively. It indicated that the resonant coupling effect of SPP plays a crucial role in the $Au/Al_2O_3/Au$ MIM waveguide. These properties will undoubtedly facilitate the application of $Au/Al_2O_3/Au$ waveguides in designing an SPP source.

Acknowledgements This work was supported by the National Natural Science Foundation of China (Grant Nos. 60907024 and 61036011), the New Teachers' Fund for the Doctoral Program of Higher Education (No. 20100001120024), Scientific Research Foundation for the Returned Overseas Chinese Scholars, State Education Ministry.

References

1. Raether H. Surface plasmons on smooth and rough surfaces and on gratings. Berlin: Springer, 1988
2. Barnes W L, Dereux A, Ebbesen T W. Surface plasmon subwavelength optics. Nature, 2003, 424(6950): 824–830
3. Hu F F, Yi H X, Zhou Z P. Wavelength demultiplexing structure based on arrayed plasmonic slot cavities. Optics Letters, 2011, 36 (8): 1500–1502
4. Hossieni A, Massoud Y H. A low-loss metal-insulator-metal plasmonic bragg reflector. Optics Express, 2006, 14(23): 11318–11323
5. Hu F F, Yi H X, Zhou Z P. Band-pass plasmonic slot filter with band selection and spectrally splitting capabilities. Optics Express, 2011, 19(6): 4848–4855
6. Tanaka K, Tanaka M. Simulations of nanometric optical circuits based on surface plasmon polariton gap waveguide. Applied Physics Letters, 2003, 82(8): 1158–1160
7. Liu L, Han Z, He S. Novel surface plasmon waveguide for high integration. Optics Express, 2005, 13(17): 6645–6650
8. Dionne J A, Lezec H J, Atwater H A. Highly confined photon transport in subwavelength metallic slot waveguides. Nano Letters, 2006, 6(9): 1928–1932
9. Chen L, Shakya J, Lipson M. Subwavelength confinement in an integrated metal slot waveguide on silicon. Optics Letters, 2006, 31 (14): 2133–2135
10. Verhagen E, Dionne J A, Kuipers L K, Atwater H A, Polman A. Near-field visualization of strongly confined surface plasmon polaritons in metal-insulator-metal waveguides. Nano Letters, 2008, 8(9): 2925–2929
11. Dionne J A, Sweatlock L A, Atwater H A, Polman A. Plasmon slot waveguides: towards chip-scale propagation with subwavelength-scale localization. Physical Review B: Condensed Matter and Materials Physics, 2006, 73(3): 035407
12. Yun B F, Hu G H, Cui Y P. Theoretical analysis of a nanoscale plasmonic filter based on a rectangular metal-insulator-metal waveguide. Journal of Physics D, Applied Physics, 2010, 43(38): 385102
13. Hryciw A, Jun Y C, Brongersma M L. Plasmonics: electrifying plasmonics on silicon. Nature Materials, 2010, 9(1): 3–4
14. Miyazaki H T, Kurokawa Y. Squeezing visible light waves into a 3-nm-thick and 55-nm-long plasmon cavity. Physical Review Letters, 2006, 96(9): 097401
15. Zhou J, Hu M, Zhang Y X, Zhang P, Liu W H, Liu S G. Numerical analysis of electron-induced surface plasmon excitation using the FDTD method. Journal of Optics, 2011, 13(3): 035003
16. Babuty A, Bousseksou A, Tetienne J P, Doyen I M, Sirtori C, Beaudoin G, Sagnes I, De Wilde Y, Colombelli R. Semiconductor surface plasmon sources. Physical Review Letters, 2010, 104(22): 226806
17. Koller D M, Hohenau A, Ditlbacher H, Galler N, Reil F, Aussenegg F R, Leitner A, List E J W, Krenn J R. Organic plasmon-emitting diode. Nature Photonics, 2008, 2(11): 684–687
18. Walters R J, van Loon R V A, Brunets I, Schmitz J, Polman A. A silicon-based electrical source of surface Plasmon polaritons. Nature Materials, 2010, 9(1): 21–25
19. Economou E N. Surface plasmons in thin films. Physical Review, 1969, 182(2): 539–554
20. Johnson P, Christy R. Optical constants of the noble metals. Physical Review B: Condensed Matter and Materials Physics, 1972, 6(12): 4370–4379
21. Park J, Kim H, Lee I M, Kim S, Jung J, Lee B. Resonant tunneling of surface plasmon polariton in the plasmonic nano-cavity. Optics Express, 2008, 16(21): 16903–16915